J Math Chem (2012) 50:703–733
DOI 10.1007/s10910-011-9919-z

ORIGINAL PAPER

Secondary structure elements in polylactic acid models

Izabella Irsai · Cornelia Majdik · Alexandru Lupan · Radu Silaghi-Dumitrescu

Received: 20 September 2011 / Accepted: 21 September 2011 / Published online: 8 October 2011

Abstract Geometry optimization results are reported on putative elements of secondary structure in decameric units of polylactic acid (PLA) analogous to those seen in protein structure—helical structures (α, π, 3_{10}) as well as a β-sheet—employing molecular mechanics, semiempirical, ab initio and density functional methods. The four possible structures of the deca-PLA are generally predicted, with all methods to be within ~15 kcal/mol of each other, with the more stable conformation varying depending on the method employed. The highest-level method employed here (M062x/6-311+G**) predicts that the α, π and 3_{10} structures have very similar energies, with π slightly favored by values within the error limits of the method; this is in contrast with results obtained with less accurate semiempirical and empirical methods, which predict larger differences and other structures as favorites. Relative energies of poly-L and poly-D,L lactic acid structures indicate the former to be energetically-favored over the latter. Three types of weak interactions appear to dictate the relative stabilities of secondary structure elements in polylactic acid structures.

Keywords Polylactic acid · Secondary structure · Molecular modeling · Noncovalent interaction · DFT

1 Introduction

Poly(lactic acid) (PLA) is a biodegradable polymer of interest for medical, pharmacological and environmental purposes [1–5]. The aliphatic polyester has a chiral carbon

Electronic supplementary material The online version of this article (doi:10.1007/s10910-011-9919-z) contains supplementary material, which is available to authorized users.

I. Irsai · C. Majdik · A. Lupan · R. Silaghi-Dumitrescu (✉)
Department of Chemistry and Chemical Engineering, Babes-Bolyai University,
11 Arany Janos str, Cluj-Napoca 400028, Romania
e-mail: rsilaghi@chem.ubbcluj.ro

center in the skeletal chain, allowing for two enantiomers: poly(L-lactic acid) (PLLA) and poly(D-lactic acid) (PDLA).

It is known that the PLA homopolymer can crystallize depending on the preparation condition in three polymorphs: α-[6–10], β-[9,11] and γ [8]. The crystal structures of these have been studied mainly by diffraction methods. *X*-ray experiments show the presence of helical chains of molecules in the crystal structure [7,12].

In the α-form two chains with 10_3 helical conformation are packed into the unit cell. Some authors suggest that there are two parallel chains in a triclinic cell [7], others that antiparallel chains are in an orthorhombic unit cell [11]. Later it was found that the conformation is distorted periodically from the regular helix owing to the interchain interactions [8] and the antiparallel chain arrangement plays an important role in the polymorphism [9]. The two helices turn left or right, respectively for PLLA and PDLA. The β-form is prepared at high drawing temperature and draw ratio. It has a frustrated structure containing three parallel chains of 3_1 helices in the trigonal unit cell [13]. The γ-form was found by the epitaxial crystallization and it is constituted by two antiparallel 3_1 helices in the monoclinic cell [8]. Another important crystal modification is created by the equimolecular mixture of PLLA and PDLA, and is known as the sc-form [14]. Six parallel chains of 3_1 helices are in the trigonal unit cell [15–22]. The packing in the crystal was also analyzed by computational chemistry. The poly(lactic acid) polymorphs were studied by rotational isomeric state model [21,23], molecular dynamics [10,11], Metropolis Monte Carlo model [23,24], molecular mechanics [10], and quantum chemical [25–27] simulations. It was thus found that the crystal structure is determined by the intermolecular interactions. The methyl group is contributing considerably to the interchain van der Waals interactions in the crystallite. The DFT calculation results indicate that the sc-form is the most energy-favorable among the four PLA forms studied: the stability order is sc > α > β > γ. Intermolecular non-conventional hydrogen bonding C^{α}–H···O(=C), $CH_3^{\cdot\cdot}$O(=C) and $CH_3^{\cdot\cdot}$O(ether) are formed in the stereocomplex crystal [28]. Molecular modeling results support the hydrogen-bonding arrangement deduced by FTIR results [29]. 10_3 helical chain conformation was analyzed opposite 3_1 helix by vibrational analysis on the α-form of PLA [24]. The experimental peak frequencies were better reproduced by the simulated frequencies of 10_3 helix than those by 3_1 helix. This confirms that the 10_3 helix describes better the α-form of PLA. A spectroscopic analysis was used to study the conformation of the helices in the stereocomplex PLA. Neither a pure 10_3 helix nor 3_1 helix could fit the experimental data perfectly, suggesting a certain degree of disorder in the structure.

Computational examination of (bio)polymers employing such methods as density functional theory (DFT) or Hartree–Fock (HF) has traditionally been restricted to smaller-size models due to the large computing resources required [30–33]. The reliability of empirical methods for describing biopolymers and related structures has long been established [32–36]. The present study seeks to estimate the performance of some of the commonly used computational models in predicting accurate geometries of polymer chains. For several of these methods, this is likely to be a particularly challenging situation. First, poly(lactic acid) architectures tend to rely primarily on weak, non-covalent, interactions. Second, those methods requiring parametrization may not necessarily perform efficiently if they have not been parametrized especially

for polymers. Equally importantly, the present study aims to investigate the extent to which classical biochemical structural models, other than those previously observed in crystallites, may be feasible in PLA. Such results would hold particular relevance for solution chemistry, where it is not known to which extent the PLA chains would retain structural patterns seen in crystalline forms.

2 Methods

The present study employs structures resulted from esterification of 10 lactic acid units, leading to a linear polymeric chain hereafter referred to as LA_{10}. These models were built in the Hyperchem [37] software package using built-in options of the Editor module for creating helical structures (α, π and 3_{10}) as well as a β-sheet. Geometry optimizations were performed either in vacuum or with the CPCM continuum solvent model as implemented in Gaussian09 software package [38]. Molecular mechanics calculations the UFF force field as implemented in Gaussian09 [38]. The semiempirical PM6 method was employed as implemented in the Gaussian09 [38] (labelled PM6-G in text) and MOPAC [39] (labeled PM6-M in text) software packages.

HF/3-21G* and density functional theory (M062X) computations were performed in Gaussian09 [38]. The CPCM solvation model was employed for HF and DFT calculations [38,40]. Standard convergence criteria as defined in the respective software packages were employed.

3 Results and discussion

A model for poly(lactic acid) consisting in ten repeating units, hereafter referred to as the PLA decamer was employed throughout the study. Four secondary-type structures were considered of decameric units of PLA: helical structures (α, π and 3_{10}) and β-sheet. These structures were built for the poly(L-lactic acid) (PLLA)as well as for the copolymer of poly(DL-lactic acid) (PDLLA). Reported in the Tables shown here are the energies, the helix length and the weak interactions presents in these structures. Figures 1 and 2 illustrate the optimized geometries.

3.1 Energy

The calculated relative energies for the PLLA and PDLLA structures are listed in Tables 1 and 2, respectively; absolute values are given in Supporting Information Tables S1 and S2. Comparing the calculated energy of PLLA with the energy of PDLLA it can be observed that the values in the case of PLLA are generally smaller (Table 2), suggesting that such structures are more stable. The relative energies are all within 26 kcal/mol except those made with molecular mechanics method.

The computational prediction on most stable secondary structure motif of those in Table 1 depends significantly on the method. Thus, an α structure is predicted at empirical level (UFF); even though the semiempirical method PM6, also predicts this same structure as more stable, the energy difference towards the least stable

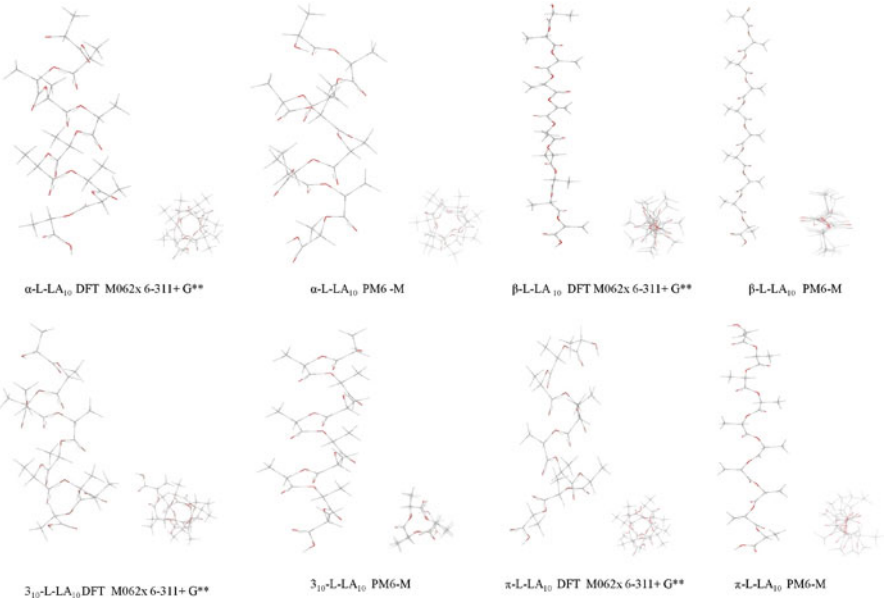

Fig. 1 Graphical representation of L-LA_{10} geometries optimized by DFT and semiempirical methods

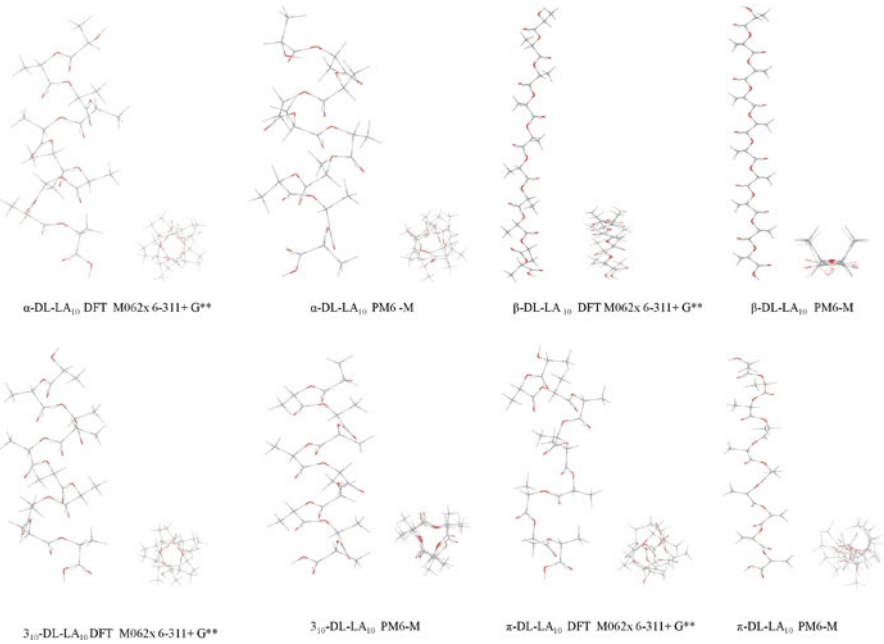

Fig. 2 Graphical representation of DL-LA_{10} geometries optimized by DFT and semiempirical methods

Table 1 The relative energies (kcal/mol)

Methods	ΔE			
	α-L-LA_{10}	π-L-LA_{10}	3_{10}-L-LA_{10}	β-L-LA_{10}
MM UFF	−68.2	0.0	−64.3	−43.7
PM6-G	−1.1	0.0	−0.8	−0.7
PM6-M	−19.1	0.0	−16.6	0.5
PM6-M solution	−3.0	0.0	−4.9	0.5
HF/3-21G*	−5.8	0.0	−8.1	−13.6
HF/3-21G* water	−1.7	0.0	*n.a.*	−12.4
HF/6-31G*	2.1	0.0	1.7	−12.5
DFT/B3LYP/6-31G*	3.5	0.0	2.9	*n.a.*
DFT/M062x/6-31G*	3.5	0.0	4.4	26.2
DFT/M062x/6-31G**	3.5	0.0	4.4	26.3
DFT/M062x/6-31G** water	0.5	0.0	0.0	18.1
DFT/M062x/6-311+G**	2.7	0.0	2.0	20.1

The energy of the π structure was taken as reference

Table 2 The relative energies (kcal/mol) of PDLLA structures, and the relative energy obtained by subtracting the energy of the PDLLA decamer from that of the PDLLA decamer

Methods	ΔE				
	α-DL-LA_{10}	π-DL-LA_{10}	3_{10}-DL-LA_{10}	β-DL-LA_{10}	DL-L
MM UFF	0.4	16.2	0.0	2.5	19.9
PM6-G	−2.3	−5.4	0.0	−8.3	−4.6
PM6-M	−0.8	20.5	0.0	26.1	2.8
PM6-M solution	0.8	5.6	0.0	8.9	5.4
HF/3-21G*	0.2	3.2	0.0	13.2	18.7
HF/3-21G* water	0.1	0.4	0.0	3.5	13.8
HF/6-31G*	0.9	−0.3	0.0	1.5	28.8
DFT/B3LYP/6-31G*	22.0	23.1	n.a.	0.0	−4.7
DFT/M062x/6-31G*	0.9	−4.4	0.0	21.2	8.9
DFT/M062x/6-31G**	1.0	−4.6	0.0	21.6	8.5
DFT/M062x/6-31G** water	7.3	7.9	0.0	21.5	0
DFT/M062x/6-311+G**	1.6	4.4	0.0	19.6	41.3

structure ranges from ∼70 kcal/mol in the molecular mechanics results to 1 kcal/mol in the PM6-G results. Interestingly, for the PM6-M method the relative order of the energies differs between the vacuum and solvated structures, hinting towards an essential role of the environment polarity in dictating the preference towards one or another type of secondary structure.

The trends seen at the HF/3-21G** level for PLLA energies differ further from those seen at empirical and semiempirical level, including the fact that solvation no

longer changes trends in relative energies, by contrast to the PM6 results. Notably, the trends further differ when comparing HF/3-21G** with 6-31G**, suggesting a strong influence of the basis set on this parameter.

The DFT results, which include some with a larger basis set with diffuse functions, may arguably be expected to provide the most reliable data of the methods shown in Table 1. Remarkably, regardless of the functional, basis set and solvation, the most stable of the four structures examined is now the π helix, and the least stable is the β sheet. This convergence towards the same trend suggests more reliability in the DFT data. However, in this case one must note that the empirical and semiempirical data yields significantly different data, disagreeing with the DFT by 20–60 kcal/mol in predicting the more stable secondary structure of those examined in the present study.

For the DFT data on the PLLA structures, we note that solvation in water tends to reduce the energy differences between the four structural motifs examined here, reversing the order between two of the structures (α and 3_{10}) but not the prediction on the most stable and least stable structures. Expanding from a double-zeta basis set to a triple-zeta one with diffuse functions does not change the trends in relative energies, although it does slightly reduce the energy differences between the four structures.

For the PDLLA structures the same disagreement may be noted as for the PLLA ones, between empirical, semiempirical and ab initio methods, as seen in Table 2. At the DFT level, where the 3_{10} structure was less stable than the π by 2–4 kcal/mol for PLLA, PDLLA shows a change in preference for 3_{10} at the highest level examined in Table 2 (M062x/6-311+G**). Also worth noting is the difference between the two functional, M06 and B3LYP, in predicting relative stabilities of the π and β structures: the predictions made by the two methods differ by ∼40 kcal/mol.

3.2 Chain length

The length of the decameric chain was measured between the ester oxygen atoms of the first monomer and the ester oxygen atoms of the ninth monomer (numbering starting from the OH terminus of the polylactide). These lengths are shown in Table 5 for PLLA.

All the methods preserve the helix length of α-L-LA_{10} within ±1.5Å of the initial structure.

The π-L-LA_{10} helix lengths obtained with HF and DFT methods drop from 21.6 Å in the initial structure to 12.1–14.2Å, suggesting convergence towards an α-type structure. By contrast, MM and PM6 methods elongate the π helix by 2.4–3.8Å compared to the starting "canonical" structure.

In the case of 3_{10}-L-LA_{10} the helix lengths predicted by all methods are similar to each other, shorter than in the initial structure and again close to the value seen in the α structure.

In terms of methodology, we note that solvation has a small effect on the helix length in all three structures (elongation by up to 0.5 Å, i.e. up to ∼5% change in helix length) (Table 3).

Table 4 shows the helix lengths of PDLLA, which appear qualitatively similar to those seen in Table 5 for PLLA. Thus, as in the case of α-L-LA_{10} the helix length of

Table 3 The helix lengths of PLLA

Methods	Helix length(Å)					
	α-L-LA_{10}		π-L-LA_{10}		3_{10}-L-LA_{10}	
	Initial	Optimized	Initial	Optimized	Initial	Optimized
MM UFF	12.4	12.3	21.6	24.0	16.0	12.1
PM6-G	12.4	12.7	21.6	25.4	16.0	14.4
PM6-M	12.4	10.9	21.6	24.6	16.0	14.0
PM6-M solution	12.4	11.4	21.6	24.5	16.0	12.3
HF/3-21G*	12.4	12.6	21.6	16.7	16.0	12.7
HF/3-21G* water	12.4	13.8	21.6	16.2	16.0	n.a.
HF/6-31G*	12.4	13.9	21.6	14.2	16.0	14.3
DFT/B3LYP/6-31G*	12.4	13.3	21.6	14.0	16.0	13.9
DFT/M062x/6-31G*	12.4	12.0	21.6	12.1	16.0	12.1
DFT/M062x/6-31G**	12.4	12.0	21.6	12.1	16.0	12.0
DFT/M062x/6-31G** water	12.4	12.3	21.6	12.6	16.0	12.5
DFT/M062x/6-311+G**	12.4	12.1	21.6	12.2	16.0	11.4

Table 4 The helix lengths of PDLLA

Methods	Helix length(Å)					
	α-DL-LA_{10}		π-DL-LA_{10}		3_{10}-DL-LA_{10}	
	Initial	Optimized	Initial	Optimized	Initial	Optimized
MM UFF	12.4	12.7	21.6	23.9	16.0	11.6
PM6-G	12.4	12.5	21.6	14.6	16.0	13.3
PM6-M	12.4	10.8	21.6	24.2	16.0	13.1
PM6-M solution	12.39	12.0	21.6	23.9	16.0	13.7
HF/3-21G*	12.4	12.7	21.6	16.6	16.0	12.8
HF/3-21G* water	12.4	13.2	21.6	16.9	16.0	13.3
HF/6-31G*	12.4	14.4	21.6	14.9	16.0	14.4
DFT/B3LYP/6-31G*	12.4	13.7	21.6	17.4	16.0	n.a.
DFT/M062x/6-31G*	12.4	12.4	21.6	7.8	16.0	12.3
DFT/M062x/6-31G**	12.4	12.3	21.6	7.8	16.0	12.2
DFT/M062x/6-31G** water	12.4	12.8	21.6	10.8	16.0	14.1
DFT/M062x/6-311+G**	12.4	12.3	21.6	13.7	16.0	12.4

α-DL-LA_{10} doesn't change much from the initial values. Also similarly to the PLLA case, there are two kinds of results by the optimization of π-DL-LA_{10}. The MM and PM6 methods induced helix lengths are longer with ∼2.5Å, while HF and DFT metods lead to shorter helices. In fact, M062x/6-31G* predicts a helix length decrease to almost one third of the initial value.

Table 5 $CO\cdots(CH)_{n+1}$ lengths for α-L-LA_{10}

O–H[a]	MM UFF	PM6-G	PM6-M	PM6-M water	HF 3-21G*	HF 3-21G* water	HF 6-31G*	DFT B3LYP 6-31G*	DFT M062x 6-31G*	DFT M062x 6-31G**	DFT M062x 6-31G** water	DFT M06/2x 6-311+G**
1-2	2.55	2.34	2.30	2.33	2.37	2.57	2.44	2.41	2.40	2.39	2.44	2.39
2-3	2.56	2.28	2.28	2.32	2.53	2.57	2.45	2.41	2.49	2.49	2.49	2.48
3-4	2.55	2.30	2.30	2.30	2.30	2.58	2.44	2.43	2.41	2.40	2.45	2.43
4-5	2.59	2.24	2.26	2.28	2.40	2.55	2.44	2.42	2.42	2.41	2.45	2.44
5-6	2.54	2.31	2.27	2.29	2.30	2.57	2.44	2.42	2.44	2.43	2.44	2.48
6-7	2.59	2.32	2.32	2.34	2.45	2.58	2.44	2.43	2.46	2.45	2.46	2.46
7-8	2.54	2.31	2.30	2.34	2.31	2.61	2.43	2.39	2.46	2.45	2.46	2.38
8-9	2.59	2.30	2.27	2.38	2.38	2.65	2.44	2.28	2.42	2.42	2.49	2.42
9-10	2.55	2.31	2.30	2.42	2.47	2.73	2.50	2.25	2.29	2.29	2.52	2.52

[a] lactic acids whose $CO\cdots(CH)_{n+1}$ lengths are indicated in this column. The initial value was 2.78 Å for all distances

The effect of solvation is somewhat larger in PDLLA than in PLLA (up to ∼3 Å, or ∼30%).

3.3 Weak interactions

In terms of the non-covalent interactions dictating secondary structure preferences in poly(lactic acid), three kinds of intramolecular interactions can be expected in the models employed in the present study.

One of these weak interactions may involve the oxygen atom of the carbonyl group and the hydrogen atom from the main chain ($CO\cdots(CH)_{n+1}$). These $CO\cdots(CH)_{n+1}$ distances in the initial structures are between 2.75 and 2.90Å, all of which exceed the 2.72 Å represented by the sum of the atomic van der Waals radii for the hydrogen and oxygen. However, after geometry optimization these distances are less than 2.72 Å in all models; the average values are between 2.34 Å and 2.45 Å, implying attractive interactions even in the β structure (Tables 5, 6, 7, 8). The differences between values predicted by various methods for the same type of secondary structure range between 0.01 and 0.3 Å. The PM6 method implemented by Mopac lead to the shortest values in all four structures. As a general rule, solvation leads to slight elongation in the O–H distances, whether computed by the semiempirical or DFT methods. One may also note that the O–H distances within the same structure are inhomogeneous.

The $CO\cdots(CH)_{n+1}$ distances measured in optimized DL-helices show two kinds of values, due to the alternating D and L isomers. The distance between the oxygen atom of an odd-numbered unit carbonyl group and next unit hydrogen atom is longer than the sum of van der Waals radii by 1 Å. After geometry optimization, only the distances between oxygen atoms of even-numbered units' carbonyl groups and next units hydrogen atoms of the main chain are shorter than 2.72 Å, effectively implying that in PDLLA there are ∼half as many O–H interactions compared to PLLA (Tables 9, 10, 11, 12).

One interesting parameter to follow, from the point of view of defining secondary structure elements, is the close contact $CO\cdots(–O–)_{n+x}$, representing distances between oxygen atoms from carbonyl groups and oxygen atoms from the ester groups. The poly(lactic acid) polymer is similar to a polypeptide, except that the peptide bonds are now replaced by ester bonds. The polypeptide chain is stabilized by intramolecular hydrogen-bonds involving precisely the peptidic atoms, N(H) and O. The equivalents of these N–O distances are listed in Tables 13, 14, 15, 16; despite the repulsive interaction that one may have expected for a CO–O situation, these distances are, even with some of the more accurate DFT methods, at the limit of the sum of van der Waals radii (3.04 Å).

The third type of non-covalent interaction involves the oxygen atoms from carbonyl groups and the hydrogen atoms from the methyl groups. For α-L-LA_{10} (Table 17) distances adequate to hydrogen bonding are provided by HF/3-21G** and by DFT methods; the nearest value to the initial structure was provided by B3LYP/6-31G*d. MM and and HF/6-31G*, yield O–H distances longer than 2.72Å. The semiempirical PM6 yields structures where only some of the CO···CH3 interactions are below the

Table 6 $CO\cdots(CH)_{n+1}$ length for π -L-LA_{10}

O–H[a]	MM UFF	PM6-G	PM6-M	PM6-M water	HF3-21G*	HF 3-21G* water	HF 6-31G*	DFT B3LYP 6-31G*	DFT M062x 6-31G*	DFT M062x 6-31G**	DFT M062x 6-31G** water	DFT M06/2x 6-311+G**
1-2	2.44	2.41	2.28	2.29	2.44	2.44	2.45	2.44	2.41	2.39	2.48	2.45
2-3	2.44	2.37	2.28	2.30	2.31	2.35	2.41	2.35	2.43	2.42	2.46	2.42
3-4	2.45	2.38	2.29	2.30	2.47	2.41	2.41	2.30	2.43	2.42	2.49	2.47
4-5	2.45	2.38	2.29	2.29	2.32	2.44	2.43	2.36	2.43	2.42	2.47	2.44
5-6	2.44	2.38	2.29	2.30	2.48	2.36	2.45	2.40	2.51	2.50	2.51	2.48
6-7	2.45	2.38	2.30	2.30	2.32	2.41	2.46	2.40	2.46	2.45	2.51	2.46
7-8	2.45	2.38	2.29	2.31	2.48	2.45	2.42	2.35	2.39	2.39	2.52	2.38
8-9	2.43	2.38	2.29	2.30	2.32	2.35	2.30	2.26	2.40	2.40	2.30	2.43
9-10	2.35	2.30	2.27	2.32	2.48	2.47	2.55	2.54	2.59	2.59	2.59	2.54

[a] lactic acids whose $CO\cdots(CH)_{n+1}$ lengths are indicated in this column. The initial value was 2.79 Å for all distances

Table 7 $CO\cdots(CH)_{n+1}$ length for 3_{10}-L-LA_{10}

O–H[a]	MM UFF	PM6-G	PM6-M	PM6-M water	HF 3-21G*	HF 3-21G* water	HF 6-31G*	DFT B3LYP 6-31G*	DFT M062x 6-31G*	DFT M062x 6-31G**	DFT M062x 6-31G** water	DFT M06/2x 6-311+G**
1-2	2.54	2.31	2.31	2.31	2.37	n.a.	2.44	2.42	2.41	2.39	2.48	2.41
2-3	2.56	2.38	2.37	2.34	2.53	n.a.	2.45	2.42	2.48	2.48	2.47	2.45
3-4	2.59	2.31	2.29	2.28	2.32	n.a.	2.44	2.43	2.40	2.39	2.47	2.46
4-5	2.55	2.31	2.29	2.28	2.41	n.a.	2.43	2.40	2.41	2.40	2.45	2.42
5-6	2.58	2.31	2.29	2.28	2.28	n.a.	2.44	2.41	2.41	2.40	2.46	2.38
6-7	2.55	2.31	2.29	2.28	2.45	n.a.	2.46	2.41	2.46	2.45	2.47	2.43
7-8	2.64	2.31	2.30	2.28	2.32	n.a.	2.42	2.36	2.43	2.42	2.46	2.36
8-9	2.61	2.28	2.29	2.32	2.36	n.a.	2.29	2.25	2.34	2.33	2.48	2.42
9-10	2.52	2.34	2.35	2.44	2.53	n.a.	2.50	2.50	2.36	2.35	2.45	2.43

[a] lactic acids whose $CO\cdots(CH)_{n+1}$ lengths are indicated in this column. The initial value was 2.90 Å for all distances

Table 8 $CO\cdots(CH)_{n+1}$ length for β -L-LA_{10}

O–H[a]	MM UFF	PM6-G	PM6-M	PM6-M water	HF3-21G*	HF 3-21G* water	HF 6-31G*	DFT B3LYP 6-31G*	DFT M062x 6-31G*	DFT M062x 6-31G**	DFT M062x 6-31G** water	DFT M06/2x 6-311+G**
1-2	2.50	2.41	2.27	2.29	2.54	2.49	2.49	*n.a.*	2.38	2.38	2.38	2.38
2-3	2.50	2.37	2.30	2.28	2.53	2.55	2.48	*n.a.*	2.37	2.37	2.39	2.37
3-4	2.50	2.38	2.27	2.28	2.53	2.56	2.48	*n.a.*	2.38	2.38	2.39	2.39
4-5	2.50	2.38	2.29	2.28	2.54	2.56	2.48	*n.a.*	2.38	2.37	2.39	2.38
5-6	2.49	2.38	2.29	2.28	2.53	2.55	2.48	*n.a.*	2.38	2.39	2.38	2.39
6-7	2.50	2.38	2.29	2.28	2.53	2.55	2.48	*n.a.*	2.37	2.36	2.39	2.37
7-8	2.50	2.38	2.30	2.27	2.54	2.56	2.48	*n.a.*	2.36	2.38	2.37	2.38
8-9	2.50	2.39	2.29	2.29	2.53	2.55	2.49	*n.a.*	2.38	2.35	2.39	2.36
9-10	2.50	2.34	2.40	2.42	2.52	2.55	2.46	*n.a.*	2.37	2.37	2.39	2.37

[a] lactic acids whose $CO\cdots(CH)_{n+1}$ lengths are indicated in this column. The initial value was 2.75 Å for all distances

Table 9 $CO\cdots(CH)_{n+1}$ lengths for α -DL-LA_{10}

$CO\cdots(CH)_{n+1}$	Initial	MM UFF	PM6-G	PM6-M water	PM6-M	HF 3-21G*	HF 3-21G* water	HF 6-31G*	DFT B3LYP 6-31G*	DFT M062x 6-31G*	DFT M062x 6-31G**	DFT M062x 6-31G** water	DFT M06/2x 6-311+G**
1-2	3.82	3.85	3.88	3.88	3.75	3.81	3.76	3.73	3.75	3.71	3.72	3.71	3.73
2-3	2.78	2.52	2.30	2.24	2.23	2.57	2.37	2.46	2.43	2.46	2.45	2.50	2.48
3-4	3.82	3.84	3.88	3.87	3.83	3.84	3.80	3.75	3.80	3.76	3.76	3.74	3.77
4-5	2.78	2.55	2.33	2.31	2.24	2.38	2.43	2.45	2.40	2.43	2.41	2.49	2.40
5-6	3.82	3.86	3.89	3.86	3.86	3.83	3.80	3.75	3.80	3.75	3.75	3.75	3.75
6-7	2.78	2.58	2.32	2.34	2.28	2.35	2.44	2.51	2.51	2.41	2.40	2.51	2.39
7-8	3.82	3.87	3.89	3.86	3.86	3.84	3.79	3.76	3.81	3.77	3.77	3.76	3.77
8-9	2.78	2.54	2.30	2.41	2.31	2.33	2.51	2.29	2.25	2.28	2.28	2.36	2.28
9-10	3.82	3.86	3.88	3.88	3.89	3.84	3.83	3.76	3.79	3.76	3.76	3.76	3.76

Table 10 $CO\cdots(CH)_{n+1}$ lengths for β-DL-LA_{10}

$CO\cdots(CH)_{n+1}$	Initial	MM UFF	PM6-G	PM6-M water	PM6-M	HF 3-21G*	HF 3-21G* water	HF 6-31G*	DFT B3LYP 6-31G*	DFT M062x 6-31G*	DFT M062x 6-31G**	DFT M062x 6-31G** water	DFT M06/2x 6-311+G**
1-2	2.75	2.50	2.28	2.56	2.81	2.51	2.50	2.39	2.36	2.39	2.38	2.37	2.40
2-3	2.75	2.50	2.80	2.41	2.58	2.51	2.50	2.40	2.41	2.39	2.39	2.40	2.40
3-4	2.75	2.50	2.33	2.45	2.58	2.52	2.51	2.40	2.40	2.41	2.40	2.37	2.42
4-5	2.75	2.50	2.69	2.45	2.57	2.52	2.51	2.40	2.37	2.39	2.38	2.41	2.39
5-6	2.75	2.50	2.28	2.45	2.55	2.52	2.51	2.40	2.36	2.41	2.41	2.38	2.41
6-7	2.75	2.50	2.53	2.44	2.55	2.52	2.51	2.40	2.32	2.40	2.40	2.39	2.42
7-8	2.75	2.50	2.29	2.44	2.53	2.52	2.52	2.40	2.33	2.41	2.41	2.41	2.41
8-9	2.75	2.50	2.60	2.43	2.53	2.52	2.50	2.39	2.39	2.40	2.40	2.40	2.40
9-10	2.75	2.50	2.28	2.35	2.59	2.52	2.51	2.40	2.40	2.39	2.39	2.40	2.41

Table 11 $CO\cdots(CH)_{n+1}$ lengths for π -DL-LA_{10}

$CO\cdots(CH)_{n+1}$	Initial	MM UFF	PM6-G	PM6-M water	PM6-M	HF 3-21G*	HF 3-21G* water	HF 6-31G*	DFT B3LYP 6-31G*	DFT M062x 6-31G*	DFT M062x 6-31G**	DFT M062x 6-31G** water	DFT M06/2x 6-311+G**
1-2	3.82	3.88	3.86	3.88	3.88	3.77	3.75	3.72	3.76	3.70	3.70	3.71	3.70
2-3	2.79	2.57	2.28	2.26	2.24	2.33	2.37	2.45	2.26	2.31	2.30	2.49	2.48
3-4	3.82	3.85	3.85	3.85	3.86	3.81	3.77	3.75	3.79	3.74	3.74	3.73	3.76
4-5	2.79	2.35	2.30	2.25	2.22	2.32	2.36	2.45	2.25	2.38	2.37	2.48	2.30
5-6	3.82	3.85	3.85	3.87	3.86	3.80	3.77	3.75	3.79	3.75	3.75	3.85	3.74
6-7	2.79	2.33	2.30	2.28	2.23	2.32	2.37	2.48	2.25	2.39	2.38	2.60	2.28
7-8	3.82	3.85	3.85	3.85	3.86	3.80	3.77	3.76	3.79	3.75	3.75	3.75	3.74
8-9	2.79	2.54	2.30	2.25	2.24	2.32	2.36	2.32	2.25	2.27	2.27	2.35	2.29
9-10	3.82	3.85	3.86	3.87	3.87	3.75	3.73	3.72	3.76	3.71	3.71	3.72	3.72

Table 12 $CO\cdots(CH)_{n+1}$ length for 3_{10}-DL-LA_{10}

$CO\cdots(CH)_{n+1}$	Initial	MM UFF	PM6-G	PM6-M water	PM6-M	HF 3-21G*	HF 3-21G* water	HF 6-31G*	DFT B3LYP 6-31G*	DFT M062x 6-31G*	DFT M062x 6-31G**	DFT M062x 6-31G** water	DFT M06/2x 6-311+G**
1-2	3.81	3.84	3.87	3.88	3.86	3.81	3.75	3.73	n.a.	3.71	3.71	3.74	3.71
2-3	2.90	2.55	2.33	2.33	2.37	2.57	2.37	2.46	n.a.	2.45	2.43	2.50	2.44
3-4	3.81	3.85	3.89	3.87	3.87	3.83	3.81	3.75	n.a.	3.76	3.77	3.77	3.76
4-5	2.90	2.53	2.32	2.29	2.29	2.38	2.44	2.45	n.a.	2.40	2.37	2.51	2.42
5-6	3.81	3.86	3.89	3.88	3.87	3.83	3.80	3.75	n.a.	3.76	3.76	3.77	3.77
6-7	2.90	2.58	2.32	2.32	2.28	2.34	2.49	2.50	n.a.	2.42	2.38	2.51	2.42
7-8	3.81	3.86	3.89	3.89	3.87	3.84	3.79	3.76	n.a.	3.77	3.77	3.76	3.77
8-9	2.90	2.53	2.31	2.47	2.31	2.39	2.54	2.34	n.a.	2.31	2.30	2.50	2.35
9-10	3.81	3.86	3.88	3.86	3.88	3.77	3.75	3.73	n.a.	3.73	3.73	3.75	3.73

Table 13 $CO\cdots(–O–)_{n+4}$ length for α-L-LA_{10}

$CO\cdots(–O–)_{n+4}$	Initial	MM UFF	PM6-G	PM6-M water	PM6-M	HF 3-21G*	HF 3-21G* water	HF 6-31G*	DFT B3LYP 6-31G*	DFT M062x 6-31G*	DFT M062x 6-31G**	DFT M062x 6-31G** water	DFT M06/2x 6-311+G**
1-5	3.02	3.08	3.83	3.33	3.39	3.63	3.77	3.78	3.60	2.99	2.99	3.03	3.09
2-6	3.02	3.04	3.49	3.29	3.29	4.05	3.80	3.84	3.59	2.97	2.97	3.06	3.11
3-7	3.03	3.20	4.43	3.39	3.37	3.97	3.82	3.98	3.61	3.00	2.99	3.23	3.22
4-8	3.02	2.99	4.78	3.42	3.30	4.15	3.75	3.93	3.71	2.98	2.98	3.25	3.13
5-9	3.02	3.20	4.75	3.47	3.38	3.97	3.79	3.87	3.73	3.03	3.03	3.18	3.02
6-10	3.02	2.98	4.79	3.41	3.35	4.16	3.77	4.10	3.63	3.03	3.02	3.01	2.84

Table 14 $CO\cdots(-O-)_{n+3}$ length for 3_{10}-L-LA_{10}

$CO\cdots(-O-)_{n+3}$	Initial	MM UFF	PM6-G	PM6-M water	PM6-M	HF 3-21G*	HF 3-21G* water	HF 6-31G*	DFT B3LYP 6-31G*	DFT M062x 6-31G*	DFT M062x 6-31G**	DFT M062x 6-31G** water	DFT M06/2x 6-311+G**
1-4	2.83	3.22	3.51	3.44	3.39	3.11	n.a.	3.45	3.36	3.08	3.09	3.02	3.25
2-5	2.83	3.52	3.43	3.27	3.36	3.19	n.a.	3.47	3.35	3.11	3.10	3.10	3.24
3-6	2.82	3.25	3.49	3.44	3.41	3.66	n.a.	3.50	3.38	3.14	3.14	3.10	3.06
4-7	2.83	3.56	3.47	3.31	3.38	3.34	n.a.	3.52	3.44	3.17	3.17	3.09	3.26
5-8	2.83	3.18	3.47	3.44	3.39	3.26	n.a.	3.47	3.32	3.20	3.21	3.14	3.10
6-9	2.83	3.71	3.49	3.39	3.42	3.17	n.a.	3.32	3.22	3.04	3.04	3.14	3.07
7-10	2.83	3.29	3.48	3.65	3.46	3.47	n.a.	3.56	3.58	3.10	3.11	3.06	4.43

Table 15 $CO\cdots(–O–)_{n+4}$ length for α-DL-LA_{10}

$CO\cdots(–O–)_{n+4}$	Initial	MM UFF	PM6-G	PM6-M water	PM6-M	HF 3-21G*	HF 3-21G* water	HF 6-31G*	DFT B3LYP 6-31G*	DFT M062x 6-31G*	DFT M062x 6-31G**	DFT M062x 6-31G** water	DFT M06/2x 6-311+G**
1-5	3.02	2.93	3.62	3.41	3.51	3.97	3.78	4.09	3.62	3.22	3.20	3.28	3.36
2-6	3.02	2.99	4.30	3.33	3.11	3.43	3.95	4.20	3.75	3.09	3.06	3.38	3.09
3-7	3.03	2.91	4.01	3.36	3.13	3.89	3.80	4.27	4.01	3.10	3.13	3.30	3.25
4-8	3.02	3.46	4.27	4.03	3.22	4.03	3.95	4.60	4.34	3.16	3.13	3.41	3.15
5-9	3.02	2.96	3.99	3.23	3.14	3.80	3.74	4.09	3.71	3.13	3.06	3.28	3.08
6-10	3.02	4.22	4.30	3.61	4.00	3.84	4.05	3.87	3.57	3.01	3.02	3.01	3.05

Table 16 CO· · ·(–O–)n+3 length for 3_{10}-DL-LA_{10}

CO· · ·$(–O–)_{n+3}$	Initial	MM UFF	PM6-G	PM6-M water	PM6-M	HF 3-21G*	HF 3-21G* water	HF 6-31G*	DFT B3LYP 6-31G*	DFT M062x 6-31G*	DFT M062x 6-31G**	DFT M062x 6-31G** water
1-4	2.83	3.41	2.93	2.98	2.86	2.79	2.88	3.12	2.73	2.73	3.17	2.75
2-5	2.83	4.71	3.39	3.43	3.36	3.02	3.43	3.45	2.97	2.97	3.46	3.04
3-6	2.82	3.71	2.92	2.94	2.85	2.84	2.87	3.09	2.74	2.75	3.16	2.76
4-7	2.83	4.78	3.41	3.49	3.36	3.27	3.47	3.52	2.99	3.00	3.50	3.05
5-8	2.83	3.57	2.92	2.95	2.85	2.88	2.87	3.15	2.79	2.80	3.16	2.79
6-9	2.83	3.49	3.42	3.48	3.41	3.42	3.39	3.37	2.93	2.97	3.51	2.99
7-10	2.83	3.02	2.91	3.50	2.86	2.85	2.85	3.07	2.77	2.78	3.13	2.77

Table 17 $CO\cdots(CH3)_{n+3}$ length for α -L-LA_{10}. The initial value was 2.59 Å for all distances

$CO\cdots(C\underline{H}_3)_{n+3}$	MM UFF	PM6-G	PM6-M water	PM6-M	HF 3-21G*	HF 3-21G* water	HF 6-31G*	DFT B3LYP 6-31G*	DFT M062x 6-31G*	DFT M062x 6-31G**	DFT M062x 6-31G** water	DFT M06/2x 6-311+G**
1-4	2.93	4.34	2.67	2.95	2.35	2.47	2.82	2.63	2.39	2.38	2.40	2.45
2-5	3.41	3.78	2.92	3.55	2.39	2.45	2.78	2.63	2.44	2.44	2.39	2.45
3-6	2.82	2.30	2.93	3.34	2.37	2.48	2.80	2.64	2.43	2.42	2.41	2.50
4-7	3.33	2.22	3.07	2.95	2.40	2.46	2.81	2.61	2.41	2.41	2.41	2.43
5-8	2.82	2.19	3.37	3.55	2.37	2.46	2.82	2.62	2.41	2.40	2.38	2.58
6-9	3.31	2.19	2.92	3.17	2.34	2.52	2.78	2.78	2.39	2.39	2.46	3.63
7-10	2.78	2.18	2.35	2.36	2.51	2.45	2.82	2.62	2.52	2.50	2.41	2.89

respective sum of van de Waals radii, illustrating irregularity. Solvation generally leads to slight elongation of these distances.

The $CO \cdots (CH_3)$ distances of optimized β-L-LA10 decamer are shown in Table 18. The only one method which yields distances corresponding to hydrogen bonding is MM.

In the initial structure of π-L-LA_{10} the $CO \cdots (CH_3)$ distances are around 7Å (Table 19). The MM and PM6 methods tend to conserve these non-bonding distances, while HF and DFT distinctly shorten them, to less than the corresponding sum of van der Waals radii.

As illustrated in Table 20, for the 3_{10}-L-La_{10} structure all methods retain carbonyl-methyl distances shorter than the sum of vand der Waals radii, with PM6 yielding the shortest contacts.

Table 21 shows $CO \cdots (CH_3)$ distances for α-DL-La_{10}. As for the other two parameters examined in the present study, there are two kinds of distances, due to the presence of the D and L isomers. Distances corresponding to hydrogen bonds are between carbonyl groups of every second units and methyl groups of n+3 units, but not all methods predict this patterns to be conserved.

Table 22 shows that in the β-DL-La_{10} structure the carbonyl-methyl distances are predicted to be distinctly longer than in the starting, protein-like structure, although with most methods values slightly shorter than the sum of van der Waals radii are retained. Notably, the values obtained with B3LYP exceed those predicted by the M06 functional by ∼1.5 Å.

The presence of $CO \cdots (CH_3)$ distance smaller than 2.72 Å is not regular in the optimized π-DL-La_{10}. The results of optimization do not follow any pattern, cf. Table 23, and differ from method to method in this respect. Shorter contacts are predicted between the carbonyl groups of odd units and hydrogen atoms of methyl groups of n+3 units by PM6-G, HF/3-21G*, HF/3-21G* in water, and by DFT/B3LYP, whereas HF/6-31G* and M062x/6-31G** in water predict such contacts between carbonyl groups of even units and hydrogen atoms of methyl groups of n+3 units.

Table 24 shows that for the 3_{10}-DL-LA_{10} structure, unlike π-DL-La_{10}, regularity is conserved. As in α-DL-LA_{10}, hydrogen bonds can be formed between the carbonyl groups of every second units and methyl groups of n+3 units.

The data shown here illustrates that protein-like secondary structure elements may be feasible in short decameric stretches of polylactic acid. Importantly, computational predictions on the relative stabilities and structural details differ significantly between empirical, semiempirical and ab initio methods. Even between two DFT methods, B3LYP and M062x, significant qualitative differences were noted for some of the structures. These observations underline significant difficulties in accurate predictions on structures whose integrity relies exclusively on weak, non-covalent interactions. Solvation, using water as solvent, appears to lead to a slight, but detectable elongation of the weak contacts.

The highest-level methods employed here predict that α, π and 3_{10} structures have very similar energies, with π slightly favored by values within the error limits of the method; this is in contrast with results obtained with less accurate semiempirical and empirical methods, which predict larger differences and other structures as favorites.

Table 18 $CO\cdots(CH3)_{n+1}$ length for β -L-LA_{10}

$CO\cdots(C\underline{H}_3)_{n+1}$	MM UFF	PM6-G	PM6-M water	PM6-M	HF 3-21G*	HF 3-21G* water	HF 6-31G*	DFT M062x 6-31G*	DFT M062x 6-31G**	DFT M062x 6-31G** water	DFT M06/2x 6-311+G**
1-2	2.62	3.39	4.66	4.43	2.95	2.84	3.44	3.55	2.73	3.55	2.78
2-3	2.62	3.19	4.98	4.73	2.93	4.43	3.34	3.37	2.79	3.47	2.82
3-4	2.62	3.17	5.51	5.18	2.92	4.45	3.36	3.44	2.75	3.48	2.77
4-5	2.62	3.17	5.53	5.10	2.91	4.44	3.36	3.39	2.76	3.47	2.79
5-6	2.62	3.17	5.48	5.07	2.91	4.44	3.36	3.41	2.76	3.47	2.79
6-7	2.62	3.17	5.49	5.06	2.91	4.44	3.36	3.36	2.83	3.44	2.82
7-8	2.62	3.16	5.53	5.24	2.93	4.67	3.37	3.39	2.75	3.46	2.80
8-9	2.62	3.23	5.47	5.37	2.95	4.44	3.38	3.44	2.86	3.50	2.88
9-10	2.62	2.98	4.69	3.82	2.95	4.44	3.33	3.35	2.75	3.43	2.79

The initial value was 2.27 Å for all distances

Table 19 $CO\cdots(CH3)_{n+3}$ length for π -L-LA_{10}

$CO\cdots(C\underline{H}_3)_{n+3}$	MM UFF	PM6-G	PM6-M water	PM6-M	HF 3-21G*	HF 3-21G* water	HF 6-31G*	DFT B3LYP 6-31G*	DFT M062x 6-31G*	DFT M062x 6-31G**	DFT M062x 6-31G** water	DFT M06/2x 6-311+G**
1-4	8.03	9.17	8.07	8.10	2.45	2.48	3.06	3.34	2.65	2.66	2.42	2.54
2-5	7.86	9.28	8.01	8.06	5.01	4.91	2.76	2.62	2.40	2.40	2.43	2.42
3-6	7.99	9.27	8.00	7.96	2.45	3.77	2.84	2.75	2.43	2.42	2.44	2.46
4-7	8.03	9.27	7.94	7.91	5.11	2.49	2.80	2.59	2.41	2.41	2.42	2.41
5-8	7.87	9.27	7.97	7.93	2.44	4.88	2.78	2.58	2.52	2.51	2.51	2.57
6-9	7.86	9.33	8.13	8.29	5.10	3.72	2.80	2.64	3.12	3.11	3.10	2.57
7-10	8.49	9.13	8.04	8.47	2.43	2.47	2.69	2.58	2.54	2.52	2.35	3.54

The initial value was 7.11 Å for all distances

Table 20 $CO\cdots(CH3)_{n+3}$ length for 3_{10}-L-LA_{10}

$CO\cdots(C\underline{H}_3)_{n+3}$	MM UFF	PM6-G	PM6-M water	PM6-M	HF 3-21G*	HF 6-31G*	DFT B3LYP 6-31G*	DFT M062x 6-31G*	DFT M062x 6-31G**	DFT M062x 6-31G** water	DFT M06/2x 6-311+G**
1-4	3.23	2.21	2.21	2.12	2.36	2.82	2.65	2.37	2.36	2.42	2.46
2-5	2.81	2.19	2.22	2.12	2.42	2.79	2.63	2.42	2.42	2.41	2.48
3-6	3.34	2.19	2.18	2.11	2.36	2.80	2.61	2.40	2.39	2.43	2.49
4-7	2.86	2.19	2.26	2.10	2.36	2.79	2.61	2.40	2.40	2.39	2.51
5-8	2.96	2.19	2.23	2.10	2.39	2.79	2.61	2.38	2.38	2.41	2.63
6-9	3.55	2.19	2.24	2.10	2.38	2.85	2.66	2.51	2.50	2.49	4.30
7-10	2.74	2.19	2.25	2.17	2.39	2.70	2.61	2.40	2.39	2.42	3.64

The initial value was 2.93 Å for all distances

Table 21 $CO\cdots(CH3)_{n+3}$ length for α -DL-LA_{10}

$CO\cdots(C\underline{H}_3)_{n+3}$	Initial	MM UFF	PM6-G	PM6-M water	PM6-M	HF 3-21G*	HF 3-21G* water	HF 6-31G*	DFT B3LYP 6-31G*	DFT M062x 6-31G*	DFT M062x 6-31G**	DFT M062x 6-31G** water	DFT M06/2x 6-311+G**
1-4	5.52	5.22	6.77	5.31	6.51	4.12	4.38	4.84	4.86	4.62	4.62	4.82	4.59
2-5	2.59	3.28	2.18	2.23	4.48	2.41	2.54	2.84	2.67	2.41	2.41	2.44	2.45
3-6	5.53	5.89	4.36	5.56	5.89	4.23	4.37	4.64	4.52	4.65	4.59	4.70	4.52
4-7	2.59	5.20	2.17	3.55	3.92	2.36	2.45	2.94	2.77	2.40	2.39	2.41	2.38
5-8	5.52	6.00	4.31	5.73	5.85	4.33	4.36	4.91	4.77	4.60	4.64	4.64	4.66
6-9	2.59	2.81	2.20	2.34	2.28	2.37	2.49	3.34	3.34	2.63	2.58	2.69	2.60
7-10	5.52	5.44	3.95	5.38	4.79	4.11	4.22	3.60	3.83	4.06	4.07	3.81	4.22

Table 22 $CO\cdots(CH3)_{n+1}$ length for β -DL-LA_{10}

$CO\cdots(C\underline{H}_3)_{n+1}$	MM UFF	PM6-G	PM6-M water	PM6-M	HF 3-21G*	HF 3-21G* water	HF 6-31G*	DFT B3LYP 6-31G*	DFT M062x 6-31G*	DFT M062x 6-31G**	DFT M062x 6-31G** water	DFT M06/2x 6-311+G**
1-2	2.63	3.73	2.73	2.38	2.71	2.75	2.83	4.27	2.65	2.64	2.71	2.66
2-3	2.62	2.40	3.00	2.58	2.72	2.78	2.83	4.34	2.66	2.65	2.68	2.67
3-4	2.64	4.05	2.97	2.63	2.72	2.76	2.84	2.80	2.63	2.62	2.74	2.63
4-5	2.62	2.45	2.93	2.64	2.72	2.77	2.83	2.85	2.67	2.68	2.67	2.70
5-6	2.63	3.40	2.97	2.64	2.72	2.76	2.84	4.25	2.63	2.63	2.69	2.65
6-7	2.62	2.71	2.96	2.67	2.73	2.77	2.84	4.16	2.64	2.64	2.71	2.66
7-8	2.64	3.57	2.96	2.71	2.73	2.76	2.84	4.18	2.64	2.63	2.66	2.65
8-9	2.62	2.72	3.02	2.71	2.73	2.79	2.86	4.32	2.65	2.64	2.68	2.68
9-10	2.63	3.86	3.14	2.60	2.71	2.77	2.83	2.79	2.66	2.66	2.69	2.65

The initial value was 2.27 Å for all distances

Table 23 $CO\cdots(CH3)_{n+3}$ length for π -DL-LA_{10}

$CO\cdots(C\underline{H}_3)_{n+3}$	Initial	MM UFF	PM6-G	PM6-M water	PM6-M	HF 3-21G*	HF 3-21G* water	HF 6-31G*	DFT B3LYP 6-31G*	DFT M062x 6-31G*	DFT M062x 6-31G**	DFT M062x 6-31G** water	DFT M062x 6-311+G**
1-4	6.54	6.55	2.32	6.95	7.28	2.40	2.44	4.86	2.52	5.24	5.21	4.71	4.77
2-5	7.11	6.82	6.90	8.24	7.66	5.54	5.56	2.83	6.56	6.62	6.64	2.44	2.56
3-6	6.54	7.25	2.32	7.66	7.35	2.40	2.44	4.68	2.56	4.56	4.57	5.18	2.63
4-7	7.11	7.61	7.10	7.13	7.48	5.46	5.70	2.91	5.94	2.34	2.33	2.32	5.19
5-8	6.54	6.85	2.32	6.69	7.30	2.41	2.44	4.80	2.57	4.75	4.73	6.67	2.40
6-9	7.11	9.04	7.07	8.66	8.04	5.42	5.57	2.90	5.87	2.55	2.53	2.71	5.59
7-10	6.54	7.34	2.29	7.94	7.83	2.39	2.43	2.91	2.57	2.49	2.49	2.75	2.42

Table 24 $CO\cdots(CH3)_{n+3}$ length for 3_{10}-DL-LA_{10}

$CO\cdots(C\underline{H}_3)_{n+3}$	Initial	MM UFF	PM6-G	PM6-M water	PM6-M	HF 3-21G*	HF 3-21G* water	HF 6-31G*	DFT M062x 6-31G*	DFT M062x 6-31G**	DFT M062x 6-31G** water	DFT M06/2x 6-311+G**
1-4	4.25	5.85	4.30	4.78	4.40	4.10	4.38	4.84	4.68	4.67	5.17	4.65
2-5	2.93	5.10	2.19	2.16	2.11	2.40	2.54	2.84	2.39	2.40	2.90	2.39
3-6	4.25	6.04	4.32	4.58	4.32	4.23	4.38	4.65	4.51	4.51	5.14	4.58
4-7	2.93	5.18	2.18	2.21	2.13	2.36	2.45	2.91	2.37	2.35	2.94	2.39
5-8	4.25	5.99	4.32	4.62	4.41	4.34	4.38	4.91	4.62	4.62	5.13	4.53
6-9	2.93	2.79	2.18	2.16	2.14	2.33	2.52	3.02	2.50	2.48	2.99	2.57
7-10	4.25	5.50	4.15	5.21	4.30	4.10	4.08	3.66	4.04	4.12	5.02	4.00

Relative energies of poly-L and poly-D,L lactic acid structures indicate the former to be energetically-favored over the latter.

The details of structural features predicted by empirical, semiempirical and ab initio methods also differ in some of the cases. Three types of weak interactions appear to dictate the relative stabilities of secondary structure elements in polylactic acid structures. These non-covalent interactions involve the oxygen atom of the carbonyl group and atoms of neighboring monomers in the primary structure, as follows: (1) the hydrogen atom of the CH group in lactic acid, (2) a hydrogen atom in the methyl group, and (3) the oxygen atom of an ester group.

For studies analogous to the present one, where several methods are used simultaneously, we suggest a simple mathematical tool to represent the results where the methodological variations often hide the essential elements of the findings. We use the present data and terminology; however, the technique can be easily generalized.

Taking the initial data obtained with method m as $L_{i,m}$, and the optimized value as $L_{opt,m}$, the variations of helix length of PLLA can be characterized by the quantity

$$Q_m = L_{opt,m} - L_{i,m}, \tag{1}$$

and by the weighted average Q_{wav},

$$Q_{wav} = \left(1/ \sum_{(m=1,n)w_m} \right) \sum_{(m=1,n)} w_m |Q_m| \tag{2}$$

where the w_m weights represent a reliability scale for the individual methods m, falling within the [0,1] interval:

$$0 \leq w_m \leq 1. \tag{3}$$

It is customary in many current studies to make a choice for the most reliable method, and ignore the other results, which in the present scheme would correspond to choosing one of the weights as unity and all the others as zero, however, this approach might be less than satisfactory. We may also take this approach, however, in a future study on a wider range of compounds we plan to suggest values for these w_m quantities. Indeed, our preliminary data on peptide structures of various natures suggest it imperative for such an approach to be implemented.

Acknowledgments This work was supported by CNCSIS-UEFISCDI, projects PNII—ID 312/2008 (to RSD and AL), project Parteneriate 72152/2008 (to CM) and by a PhD scholarship from Contract POSDRU/88/1.5/S/60185—"Innovative doctoral studies in a knowledge based society" (to II). We wish to acknowledge the work of Dr. Eng. Attila Kun at UBB for maintenance of our computational facilities.

References

1. Y. Hu, X. Jiang, Y. Ding, L. Zhang, C. Yang, J. Zhang, Biomaterials **24**, 2395 (2003)
2. T. Ouchi, T. Saito, T. Kontani, Y. Ohya, Macromol. Biosci. **4**, 458 (2004)
3. M.E.I. Baseir, I.W. Kellaway, Int. J. Pharmacol. **175**, 135 (1998)

4. T. Chandy, G.S. Das, R.F. Wilson, G.H.R. Rao, J. Appl. Polym. Sci. **86**, 1285 (2002)
5. A. Viinikainen, H. Goransson, K. Huovinen, M. Kellomaki, P. Tormala, P. Rokkanen, J. Mater. Sci. Mater. Med. **17**, 169 (2006)
6. T. Miyata, T. Masuko, Polymer **38**, 4003 (1997)
7. J. Kobayashi, T. Asahi, M. Ichiki, A. Okikawa, H. Suzuki, T. Watanabe, E. Fukada, Y. Shikinami, J. Appl. Phys. **77**, 2957 (1995)
8. W. Hoogsteen, A.R. Postema, A.J. Pennings, G.G. ten Brinke, P. Zugenmaier, Macromolecules **23**, 634 (1990)
9. S. Sasaki, T. Asakura, Macromolecules **36**, 8385 (2003)
10. D. Brizzolara, H.J. Cantow, K. Diederichs, E. Keller, A.J. Domb, Macromolecules **29**, 191 (1996)
11. C. Aleman, B. Lotz, J. Puiggali, Macromolecules **34**, 4795 (2001)
12. P. De Santis, J. Kovacs, Biopolymers **6**, 299 (1968)
13. J. Puiggali, Y. Ikada, H. Tsuji, L. Cartier, T. Okihara, B. Lotz, Polymer **41**, 8921 (2000)
14. T. Okihara, M. Tsuji, A. Kawagushi, K.I. Katayama, H. Tsuji, S.H. Hyon, Y. Ikada, J. Macromol. Sci. Phys. B **30**, 119 (1991)
15. L. Cartier, T. Okihara, Y. Ikada, H. Tsuji, J. Puiggali, B. Lotz, Polymer **41**, 8909 (2000)
16. Y. Ikada, K. Jamshidi, H. Tsuji, S.H. Hyon, Macromolecules **20**, 904 (1987)
17. H. Tsuji, Macromol. Biosci. **5**, 569 (2005)
18. H. Tsuji, Y. Ikada, Polymer **40**, 6699 (1999)
19. H. Tsuji, I. Fukui, Polymer **44**, 2891 (2003)
20. D. Sawai, Y. Tsugane, M. Tamada, T. Kanamoto, M. Sungil, S.H. Hyon, J. Polym. Sci. Part B Polym. Phys. **45**, 2632 (2007)
21. N. Rahman, T. Kawai, G. Matsuba, K. Nishida, T. Kanaya, H. Watanabe, H. Okamoto, M. Kato, A. Usuki, M. Matsuda, K. Nakajima, N. Honma, Macromolecules **42**, 4739 (2009)
22. J. Zhang, K. Tashiro, H. Tsuji, A.J. Domb, Macromolecules **40**, 1049 (2007)
23. S. Kang, S.L. Hsu, H.D. Stidham, B.P. Smith, A. Leugers, X. Yang, Macromolecules **34**, 4542 (2001)
24. K. Aou, S.L. Hsu, Macromolecules **39**, 3337 (2006)
25. J. Blomqvist, L.O. Pietila, B. Mannfors Polym. **42**, 109 (2001)
26. J. Blomqvist, Polymer **42**, 3515 (2001)
27. T.T. Lin, X.Y. Liu, C. He, J. Phys. Chem. B **114**, 3133 (2010)
28. T.T. Lin, X.Y. Liu, C. He, Polymer **51**, 2779 (2010)
29. J.R. Sarasua, N.L. Rodriguez, A.L. Arraiza, E. Meaurio, Macromolecules **38**, 8362 (2005)
30. L. Noodleman, T. Lovell, W.G. Han, J. Li, F. Himo, Chem. Rev. **104**, 459 (2004)
31. P.E. Siegbahn, M.R.A. Blomberg, Chem. Rev. **100**, 421 (2000)
32. R.A. Friesner, B.D. Dunietz, Acc. Chem. Res. **34**, 351 (2001)
33. S.R. Gooding, P.J. Winn, G.A. Jones, G.G. Ferenczy, M.J. Frusher, C.A. Reynolds, J. Phys. Chem. A. **110**, 6487 (2006)
34. A. Warshel, W.W. Parson, Q. Rev. Biophys. **34**, 563 (2001)
35. A. Warshel, Acc. Chem. Res. **35**, 385 (2002)
36. E. Rosta, M. Klahn, A. Warshel, J. Phys. Chem. B **110**, 2934 (2006)
37. HyperChem(TM) Molecular modelling system, release 4.5 SGI, Hypercube; Hyperchem(TM) molecular modelling system, Release 5.01 for Windows, Hypercube, Inc. (1998)
38. M.J. Frisch, G.W. Trucks, H.B. Schlegel, G.E. Scuseria, M.A. Robb, J.R. Cheeseman, J. Montgomery, A.T. Vreven, K.N. Kudin, J.C. Burant, J.M. Millam, S.S. Iyengar, J. Tomasi, V. Barone, B. Mennucci, M. Cossi, G. Scalmani, N. Rega, G.A. Petersson, H. Nakatsuji, M. Hada, M. Ehara, K. Toyota, R. Fukuda, J. Hasegawa, M. Ishida, T. Nakajima, Y. Honda, O. Kitao, H. Nakai, M. Klene, X. Li, J.E. Knox, H.P. Hratchian, J.B. Cross, V. Bakken, C. Adamo, J. Jaramillo, R. Gomperts, R.E. Stratmann, O. Yazyev, A.J. Austin, R. Cammi, C. Pomelli, J.W. Ochterski, P.Y. Ayala, K. Morokuma, G.A. Voth, P. Salvador, J.J. Dannenberg, V.G. Zakrzewski, S. Dapprich, A.D. Daniels, M.C. Strain, O. Farkas, D.K. Malick, A.D. Rabuck, K. Raghavachari, J.B. Foresman, J.V. Ortiz, Q. Cui, A.G. Baboul, S. Clifford, J. Cioslowski, B.B. Stefanov, G. Liu, A. Liashenko, P. Piskorz, I. Komaromi, R.L. Martin, D.J. Fox, T. Keith, M.A. Al-Laham, C.Y. Peng, A. Nanayakkara, M. Challacombe, P.M.W. Gill, B. Johnson, W. Chen, M.W. Wong, C. Gonzalez, J.A. Pople, Gaussian 09, Gaussian, Inc., Wallingford, CT (2009)
39. J.J.P. Stewart, MOPAC 2009, Stewart Computational Chemistry, Version 10.153L (2009)
40. F. Eckert, A. Klamt, AIChE J. **48**, 369 (2002)